INTERNATIONAL JOURNAL FOR NUMERICAL METHODS IN FLUIDS
Int. J. Numer. Meth. Fluids 2002; **40**:655–667 (DOI: 10.1002/fld.367)

A numerical method to solve the *m*-terms of a submerged body with forward speed

W.-Y. Duan[1,*,†] and W. G. Price[2]

[1] *College of Shipbuilding Engineering, Harbin Engineering University, Harbin 150001, People's Republic of China*
[2] *School of Engineering Sciences, Ship Science, University of Southampton, Highfield, Southampton SO17 1BJ, UK*

SUMMARY

To model mathematically the problem of a rigid body moving below the free surface, a control surface surrounding the body is introduced. The linear free surface condition of the steady waves created by the moving body is satisfied. To describe the fluid flow outside this surface a potential integral equation is constructed using the Kelvin wave Green function whereas inside the surface, a source integral equation is developed adopting a simple Green function. Source strengths are determined by matching the two integral equations through continuity conditions applied to velocity potential and its normal derivatives along the control surface. After solving for the induced fluid velocity on the body surface and the control surface, an integral equation is derived involving a mixed distribution of sources and dipoles using a simple Green function and one component of the fluid velocity. The normal derivatives of the fluid velocity on the body surface, namely the *m*-terms, are then solved by this matching integral equation method (MIEM).

Numerical results are presented for two elliptical sections moving at a prescribed Froude number and submerged depth and a sensitivity analysis undertaken to assess the influence of these parameters. Furthermore, comparisons are performed to analyse the impact of different assumptions adopted in the derivation of the *m*-terms. It is found that the present method is easy to use in a panel method with satisfactory numerical precision. Copyright © 2002 John Wiley & Sons, Ltd.

KEY WORDS: *m*-terms; free-surface effects; submerged body; integral equations

1. INTRODUCTION

Although research on ship motions and sea loads experienced by ships and offshore structures excited by seaways has progressed during recent years, many problems still exist. The thing

* Correspondence to: W.-Y. Duan, College of Shipbuilding Engineering, Harbin Engineering University, Harbin 150001, People's Republic of China.
† E-mail: yanliu_h@public.hr.hl.cn

Contract/grant sponsor: Royal Society Fellowship Scheme
Contract/grant sponsor: National Natural Science Foundation of China; contract/grant number: N19802008
Contract/grant sponsor: Ministry of Education of China; contract/grant number: N199927

Received July 2000
Revised July 2001

of interest here is the interaction between steady and oscillating waves generated by a vessel with forward speed. This has not been fully solved numerically although the problem is well posed as discussed by Timman and Newman [1], Newman [2], Inglis and Price [3, 4]. Faltinsen [5] expressed the view that to make further improvements in ship motion predictions at moderate and high Froude number it is felt that one first has to study the steady-wave potential problem in more detail. The first major difficulty is to derive the steady-wave disturbance which interacts with the oscillating waves through the free surface condition and body boundary conditions as described by Newman [6]. For the body boundary condition, the main difficulty is to determine the so called *m*-terms (as expressed in Equation (5) herein and previously defined by Timman and Newman [1], and Ogilvie and Tuck [7]), because its description contains the second-order derivatives of the steady potential. Even for linear steady Kelvin waves, a totally satisfactory numerical method to obtain the *m*-terms have not been fully derived. Beck and Magee [8] found difficulties in developing a numerical difference scheme to solve for the steady potential and they therefore adopted the double-body assumption. For the double body, a robust panel method was presented by Wu [9] to determine the *m*-terms for the two-dimensional problem and by Duan [10] for the three-dimensional problem, but in neither derivation it is easy to include wave effects. Therefore, in conclusion, the *m*-terms with wave effect has not been fully solved even for the linear steady waves case. For a submerged body with forward speed, the linear free surface condition may be regarded as a reasonable boundary assumption on which to determine the steady potential. For this case, a numerical method to calculate the *m*-terms is described in this paper.

In the proposed approach herein, a control surface is introduced which surrounds the body and divides the fluid domain into two regions. In the outer region, a potential integral equation is established using Kelvin wave Green function on the control surface. In the inner region, a source integral equation using simple Green function is adopted on the control surface and body surface. The respective source strengths are found by matching the two integral equations through the continuity condition imposed on velocity potentials and their normal derivatives along the control surface. After solving for the induced fluid velocity on the body surface and control surface, under the assumption that the fluid velocity is represented by a harmonic function, an integral equation is derived containing a mixed distribution of sources and dipoles from the application of the simple Green function and one of the components of the fluid velocity. The normal derivatives of the fluid velocity on the body surface, namely the *m*-terms, are then solved. Mathematical formulations and theoretical methods describing the proposed matching integral equation method (MIEM) are given in Sections 2 and 3. Numerical procedures are described in Section 4. Numerical results and discussions are presented for two elliptic sections at a selection of Froude numbers and submerged depths in Section 5.

2. MATHEMATICAL FORMULATIONS

Let us consider an infinitely long cylinder of constant cross-section advancing in a direction perpendicular to its axis with constant velocity U. The cylinder is fully submerged at a depth h in water of infinite depth. Furthermore, as shown in Figure 1, let us introduce a reference co-ordinate system $o-xyz$ moving with the forward speed of the cylinder. The origin o lies in the plane of the calm water surface, the ox axis is positive in the direction of forward speed and the oz axis points positively upwards.

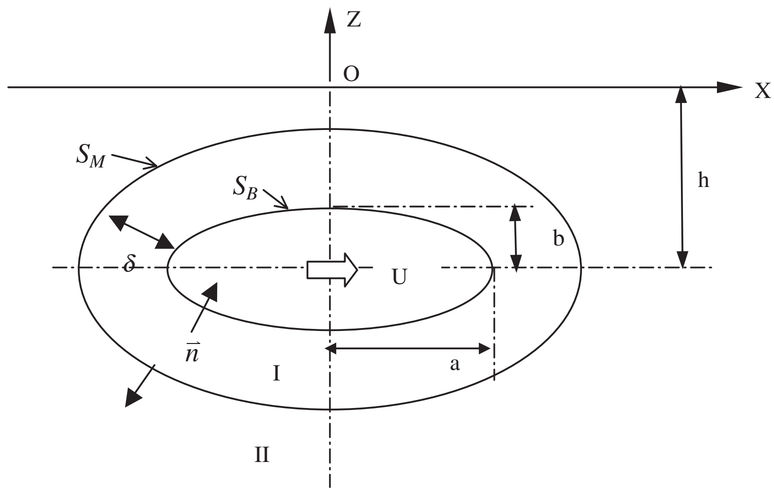

Figure 1. Illustration of an elliptical section of semi-major axis a and semi-minor axis b submerged to depth h at its centre. S_B denotes the surface of the elliptical section and S_M the boundary of a control surface.

The fluid is assumed incompressible, inviscid and the flow irrotational allowing the existence of a velocity potential $\phi(x,z)$ through the following set of equations:

(i) Based on the steady Neumann–Kelvin assumption, the velocity potential satisfies the Laplace equation

$$\frac{\partial^2\phi}{\partial x^2}+\frac{\partial^2\phi}{\partial z^2}=0 \tag{1}$$

in the whole fluid domain.

(ii) The kinematics condition on the body surface is governed by the relation

$$\frac{\partial\phi}{\partial n}=Un_x \tag{2}$$

where n_x is the component of the unit inward normal to the body in the x direction.

(iii) On the undisturbed free surface, $z=0$

$$\frac{\partial^2\phi}{\partial x^2}+v\,\frac{\partial\phi}{\partial z}=0 \tag{3}$$

where $\upsilon=g/U^2$ and g is the gravitational constant.

(iv) In water of infinite depth the condition is

$$\frac{\partial\phi}{\partial z}=0 \tag{4}$$

for $z\to-\infty$.

(v) To complete the boundary-value problem, an appropriate radiation condition is imposed. A generally accepted condition follows from the assumption that there is no wave far ahead of the body, but there are waves far behind the body (see, for example, Reference [11]).

Physically, $\phi(x,z)$ describes the steady flow and includes the steady-wave pattern created around the cylinder. In the linear ship motion theory (see, for example [2]), the steady wave is assumed small such that the steady flow interacts with the unsteady flow only through the m-terms along the body surface. These are defined as

$$(m_1,m_2,m_3) = -(\vec{n}\cdot\nabla)\vec{W}$$
$$(m_4,m_5,m_6) = -(\vec{n}\cdot\nabla)(\vec{r}\times\vec{W})$$

and are due to the oscillatory motions of the body within the steady velocity field

$$\vec{W} = \nabla(-Ux+\phi)$$

In these expressions $\vec{n}=(n_x,n_y,n_z)$ denotes the inward pointing unit normal to the body and $\vec{r}=(x,y,z)$. For the present two-dimensional case, the m-terms reduce to

$$(m_1,m_3,m_5) = -\left\{\frac{\partial^2\phi}{\partial x\partial n},\frac{\partial^2\phi}{\partial z\partial n},\left((z+h)\frac{\partial^2\phi}{\partial x\partial n}-x\frac{\partial^2\phi}{\partial z\partial n}+n_z\left(\frac{\partial\phi}{\partial x}-U\right)-n_x\frac{\partial\phi}{\partial z}\right)\right\} \tag{5}$$

For arbitrary form bodies, the m-terms create computational difficulties because of the occurrence of the second-order derivatives of the steady potential. The construction of robust numerical method of high precision to calculate the m-terms with the inclusion of the steady wave remains unsolved (or unpublished). A matching integral equation method is now discussed to alleviate this deficiency.

3. THEORETICAL METHOD

Let us first introduce a control surface S_M, which fully surrounds the body surface S_B, as shown in Figure 1. The flow region outside S_M is denoted by II and the inner region by I.

By the application of the Green theorem in the flow region II to the velocity potential $\phi^{II}(p)$ and the Green function $G(p,q)$, the integral equation defining the value of $\phi^{II}(p)$ and its normal derivative along the control surface S_M is expressed in the form

$$\pi\phi^{II}(p)+\int_{S_M}\phi^{II}(q)\frac{\partial G(p,q)}{\partial n_q}\,ds_q = \int_{S_M}G(p,q)\frac{\partial\phi^{II}(q)}{\partial n}\,ds_q \tag{6}$$

where the Green function $G(p,q)$ satisfies the same boundary condition as ϕ with the exception of the body boundary condition. Here p denotes a field point and q a source point. Wehausen and Laitone [12] expressed this function as

$$G(p,q) = \ln r_{pq} + \ln r_{p\bar{q}} + 2\,\mathrm{PV}\int_0^\infty \frac{e^{k(z+\zeta)}\cos k(x-\xi)}{k-\upsilon}\,dk + 2\pi e^{\upsilon(z+\zeta)}\sin\nu(x-\xi) \tag{7}$$

where $p=(x,z)$, $q=(\xi,\zeta)$, $r_{pq}^2=(x-\xi)^2+(z-\zeta)^2$, $r_{p\bar{q}}^2=(x-\xi)^2+(z+\zeta)^2$, and PV denotes a principle integral.

In the flow region I, following Lamb [13], a source distribution formulation using the simple Green's function $\ln r_{pq}$ is adopted to represent the velocity potential $\phi^{\mathrm{I}}(p)$ and its normal derivative along the control surface S_{M} and body surface S_{B}. That is

$$\phi^{\mathrm{I}}(p)=\int_{S_{\mathrm{M}}+S_{\mathrm{B}}}\sigma(q)\ln r_{pq}\,\mathrm{d}s_q \tag{8}$$

$$\frac{\partial\phi^{\mathrm{I}}(p)}{\partial n}=-\pi\sigma(p)+\int_{S_{\mathrm{M}}+S_{\mathrm{B}}}\sigma(q)\frac{\partial\ln r_{pq}}{\partial n_p}\,\mathrm{d}s_q \tag{9}$$

To ensure continuity along the control surface S_{M}, matching flow conditions in regions I and II gives

$$\phi^{\mathrm{I}}=\phi^{\mathrm{II}},\quad \frac{\partial\phi^{\mathrm{I}}}{\partial n}=\frac{\partial\phi^{\mathrm{II}}}{\partial n}\quad (\text{on } S_{\mathrm{M}}) \tag{10}$$

For consistency of sign convention, a positive direction is denoted by the normal vector at the control surface as shown in Figure 1. Attention has therefore to be paid to the sign of the first term on the left-hand side of Equation (6) and the right-hand side of Equation (9). Applying the matching condition to Equation (6) and using the body boundary condition described in Equation (2), we derive the necessary equations to solve for the unknown source strength $\sigma(q)$ along the surface S_{M} and S_{B}. After the completion of this calculation, the fluid velocity components on the surface S_{M} and S_{B} are subsequently determined from the equation

$$\nabla\phi^{\mathrm{I}}(p)=\int_{S_{\mathrm{M}}+S_{\mathrm{B}}}\sigma(q)\nabla_p\ln r_{pq}\,\mathrm{d}s_q \tag{11}$$

Finally, again using the Green theorem in the flow region I to the fluid velocity $\nabla\phi^{\mathrm{I}}(p)$ and the simple Green function $\ln r_{pq}$, we obtain the following boundary integral equation:

$$\int_{S_{\mathrm{M}}+S_{\mathrm{B}}}\ln r_{pq}\frac{\partial\nabla\phi^{\mathrm{I}}(q)}{\partial n}\,\mathrm{d}s_q=-\pi\nabla\phi^{\mathrm{I}}(p)+\int_{S_{\mathrm{M}}+S_{\mathrm{B}}}\nabla\phi^{\mathrm{I}}(q)\frac{\partial\ln r_{pq}}{\partial n_q}\,\mathrm{d}s_q \tag{12}$$

As the right-hand side of this equation is known from Equation (11), the second order derivative

$$\frac{\partial\nabla\phi^{\mathrm{I}}}{\partial n}=\frac{\partial\nabla\phi}{\partial n}=\left(\frac{\partial^2\phi}{\partial x\partial n},\frac{\partial^2\phi}{\partial z\partial n}\right)$$

along the surface S_{M} and S_{B} can now be solved. The m-terms are determined from Equation (5), thus completing a description of the theoretical method.

4. NUMERICAL PROCEDURES

To remain consistent with the numerical methods normally adopted to solve for the unsteady motion, a constant panel method is also used to determine the m-terms defined in Equation (5). For the present two-dimensional case, the surface S_{M} and S_{B} are approximated by NM and NB straight line segments, respectively. Over each segment, the value of

$$\phi^{\mathrm{I}}, \phi^{\mathrm{II}}, \frac{\partial \phi^{\mathrm{I}}}{\partial n}, \frac{\partial \phi^{\mathrm{II}}}{\partial n}, \sigma, \frac{\partial \phi^{\mathrm{I}}}{\partial x}, \frac{\partial \phi^{\mathrm{I}}}{\partial z}, \frac{\partial^2 \phi^{\mathrm{I}}}{\partial x\, \partial n}, \frac{\partial^2 \phi^{\mathrm{I}}}{\partial z\, \partial n}$$

assumed constant. All boundary conditions are therefore at the mid position of each segment.

Under these assumptions, the boundary integral equation (6) may be approximated by

$$\sum_{j=1}^{\mathrm{NM}} a_{ij} \phi_j^{\mathrm{II}} = \sum_{j=1}^{\mathrm{NM}} b_{ij} \frac{\partial \phi_j^{\mathrm{II}}}{\partial n} \tag{13}$$

for $i = 1, \mathrm{NM}$. Here

$$a_{ij} = \delta_{ij}\pi + \int_{\Delta S_j} \frac{\partial G_{ij}}{\partial n_j}\, \mathrm{d}s, \quad \delta_{ij} = \begin{cases} 1, & i = j, \\ 0, & i \neq j, \end{cases} \quad b_{ij} = \int_{\Delta S_j} G_{ij}\, \mathrm{d}s$$

and Equations (8) and (9) are approximated by

$$\phi_i^{\mathrm{I}} = \sum_{j=1}^{\mathrm{NM+NB}} c_{ij}\sigma_j \quad \text{for } i = 1, \mathrm{NM} + \mathrm{NB} \tag{14}$$

$$\frac{\partial \phi_i^{\mathrm{I}}}{\partial n} = \sum_{j=1}^{\mathrm{NM+NB}} d_{ij}\sigma_j \quad \text{for } i = 1, \mathrm{NM} + \mathrm{NB} \tag{15}$$

where $c_{ij} = \int_{\Delta S_j} \ln r_{ij}\, \mathrm{d}s,\ d_{ij} = -\delta_{ij}\pi + \int_{\Delta S_j} (\partial \ln r_{ij}/\partial n_i)\, \mathrm{d}s$.

By utilizing the matching condition expressed in Equation (10) on the control surface S_{M} and satisfying the body boundary condition of Equation (2) on surface S_{B}, we create a system of linear equations of the form

$$\begin{aligned} &\sum_{j=1}^{\mathrm{NM+NB}} \sum_{k=1}^{\mathrm{NM}} (a_{ik}c_{kj} - b_{ik}d_{kj})\sigma_j = 0 \quad && \text{for } i = 1, \mathrm{NM} \\ &\sum_{j=1}^{\mathrm{NM+NB}} d_{ij}\sigma_j = U n_{x,i} && \text{for } i = \mathrm{NM} + 1, \mathrm{NM} + \mathrm{NB} \end{aligned} \tag{16}$$

A Gaussian elimination process was used to solve this set of linear equations. After determining σ_j $(j = 1, \mathrm{NM} + \mathrm{NB})$ from equation (16), it is easy to solve for the fluid velocity components along the surface S_{M} and S_{B} by using the following equations:

$$\frac{\partial \phi_i^{\mathrm{I}}}{\partial x} = \sum_{j=1}^{\mathrm{NM+NB}} e_{ij}\sigma_j \quad \text{for } i = 1, \mathrm{NM} + \mathrm{NB} \tag{17}$$

$$\frac{\partial \phi_i^{\mathrm{I}}}{\partial z} = \sum_{j=1}^{\mathrm{NM+NB}} f_{ij}\sigma_j \quad \text{for } i = 1, \mathrm{NM} + \mathrm{NB} \tag{18}$$

where $e_{ij} = \int_{\Delta S_j} (\partial \ln r_{ij}/\partial x_i)\,\mathrm{d}s,\ f_{ij} = \int_{\Delta S_j} (\partial \ln r_{ij}/\partial z_i)\,\mathrm{d}s$

The second-order derivatives related to the m-terms are determined from the two systems of linear equations

$$\sum_{j=1}^{\mathrm{NM+NB}} g_{ij}\,\frac{\partial^2 \phi_i^{\mathrm{I}}}{\partial x \partial n} = \sum_{j=1}^{\mathrm{NM+NB}} h_{ij}\,\frac{\partial \phi_i^{\mathrm{I}}}{\partial x} \quad \text{for } i = 1, \mathrm{NM} + \mathrm{NB} \tag{19}$$

$$\sum_{j=1}^{\mathrm{NM+NB}} g_{ij}\,\frac{\partial^2 \phi_i^{\mathrm{I}}}{\partial z \partial n} = \sum_{j=1}^{\mathrm{NM+NB}} h_{ij}\,\frac{\partial \phi_i^{\mathrm{I}}}{\partial z} \quad \text{for } i = 1, \mathrm{NM} + \mathrm{NB} \tag{20}$$

where $g_{ij} = \int_{\Delta S_j} \ln r_{ij}\,\mathrm{d}s,\ h_{ij} = -\delta_{ij}\pi + \int_{\Delta S_j} (\partial \ln r_{ij}/\partial n_j)\,\mathrm{d}s$.

Finally by substituting the solved fluid velocity components and the second-order derivatives of the steady potential into Equation (5), we complete the construction of a numerical scheme of study to determine the m-terms on each line segment of surface S_{B}.

The proposed numerical method depends on the calculation of the influence coefficients $a_{ij}, b_{ij}, c_{ij}, d_{ij}, e_{ij}, f_{ij}, g_{ij}, h_{ij}$. Duan [14], based on results from Reference [15], derived analytical solutions for many of the integrals occurring in the definitions of the influence coefficients and the interested reader may consult this reference for details of the technique.

5. NUMERICAL RESULTS AND DISCUSSIONS

Two elliptical sections are examined to illustrate the numerical scheme of study. Figure 1 shows an elliptical section of semi-major axis a and semi-minor axis b submerged to depth h at its centre. The control surface S_{M} is also selected as an elliptical section where δ is the average normal distance between the body surface S_{B} and the control surface S_{M}.

By way of example, Figure 2 illustrates numerical calculations of the resistance of the elliptical section for a selection of slenderness ratios $a/b = 1, 2, 5$, submerged ratios $b/h = 2, 3, 4, 4.5, 5$ and forward speeds as denoted by the depth-dependent Froude number value $F_h = U/\sqrt{gh}$ from 0.4 to 2.0. In the case of $a/b = 1$(circular section), Havelock [16] presented an analytical solution for the resistance including the contribution of the velocity square terms in Bernoulli's formula. Figure 2 shows good agreement between present computations and Havelock's analytical results for $a = b$, $h = 2b$ over the chosen speed range. For $a/b = 2$ and 5 the maximum resistance corresponding to the maximum wave height occurs near $F_h = 1.0$.

To validate and demonstrate the accuracy of the numerical calculations of the m-terms, a deeply submerged body moving parallel to the ox-axis in water of infinite depth ($h \to \infty$) is examined. In this case, the analytical solution of m-terms for an ellipse is given by Lamb [13]

$$m_1 = \frac{U(a + b)(b^3 \cos^2 \theta - ba^2 \sin^2 \theta)}{(b^2 + c^2 \sin^2 \theta)^{1/2}(b^2 \cos^2 \theta + a^2 \sin^2 \theta)^2} \tag{21}$$

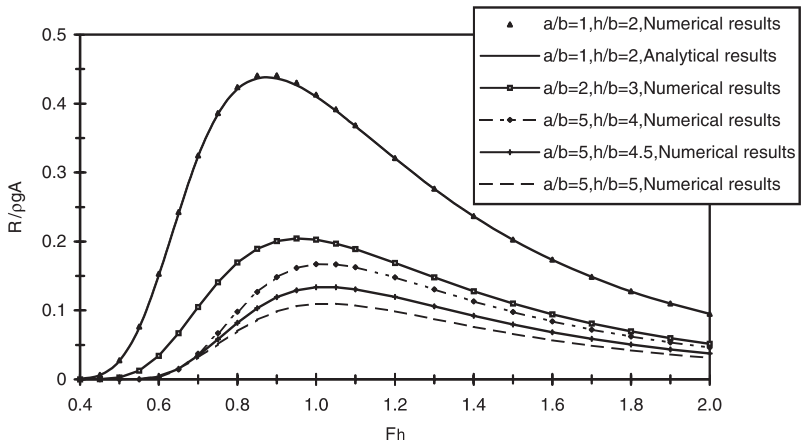

Figure 2. Wave resistance of three configurations of elliptical section at different submerged depths.

$$m_3 = \frac{U(a+b)(2ab^2 \sin\theta \cos\theta)}{(b^2 + c^2 \sin^2\theta)^{1/2}(b^2 \cos^2\theta + a^2 \sin^2\theta)^2} \tag{22}$$

and m_5 is evaluated by Equation (5). The angle θ is measured positive from the ox-axis in an anticlockwise direction. Figure 3 shows a comparison between numerical results and the analytical solution for the m-terms on the upper half surface of an ellipse of dimension $a/b = 5$. The relative error between the analytical and numerical procedures is also shown and indicates that the maximum error is less than 2% for m_1 and m_3 and less than 0.5% for m_5. It is also noticed that the minimum relative error corresponds to the maximum value of the m-terms which change very rapidly.

Two kinds of control surface S_M were examined. That is, one parallel and one non-parallel to S_B . In the former, the only variable parameter is the normal distance, δ, between S_M and S_B as shown in Figure 1. For the non-parallel case, a rectangular control surface is selected with its centre coincident with that of the ellipse. The parameter δ now indicates the nearest normal distance to the ellipse. Numerical tests show that to keep the errors less than those shown in Figure 3, the variable, δ, should be chosen such that $\delta \geqslant 0.1L$, where $L = 2a$ denotes the length of the ellipse S_B. If a large value of δ is selected, the errors reduce.

For a body submerged near the free surface, δ is selected to keep the control surface S_M within the water surface. For the results presented herein, control surface S_M is selected parallel to S_B with normal distance $\delta = 0.2a$ and segment number on S_M taken equal to that on S_B.

Figure 4 illustrates the calculated m-terms for an elliptic blunt body with dimensions $a/b = 2$ at a submerged depth $h = 3b$. Figure 5 shows similar results for an elliptic slender body with dimensions $a/b = 5$ at a submerged depth of $h = 4b$. In both cases the ellipse travels with Froude number $F_h = 0.6, 0.8, 1.0$.

The findings are compared between results in which free surface effects play a prominent role and those derived for the deeply submerged case. Although quantitative data differ

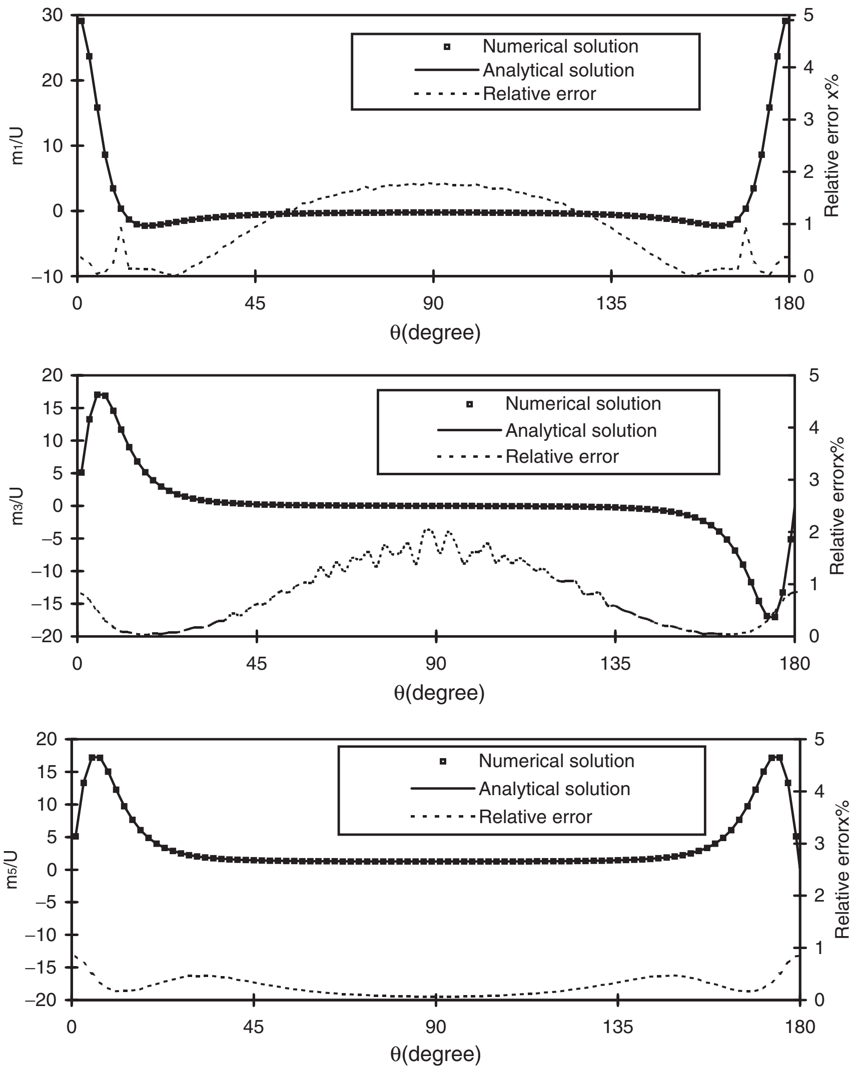

Figure 3. Comparison of m-terms between analytical and numerical results for a deeply submerged ellipse with dimension $a/b = 5$.

between respective m-terms their trends are very similar. Namely, the largest variations in the data sets occur in the regions $\theta = 0°$ and $180°$, i.e. bow and stern. The blunt body shows variation distributed over a greater surface region whereas the slender body indicates a more confined distribution with m-terms of greater magnitude. Speed influence is more noticeable over the whole surface of the blunt body whereas for the slender body its influence is only observed in the bow and stern regions. In the data presented for the m_5-terms, the simple term adopted in a strip theory and three-dimensional theory is included for illustrative

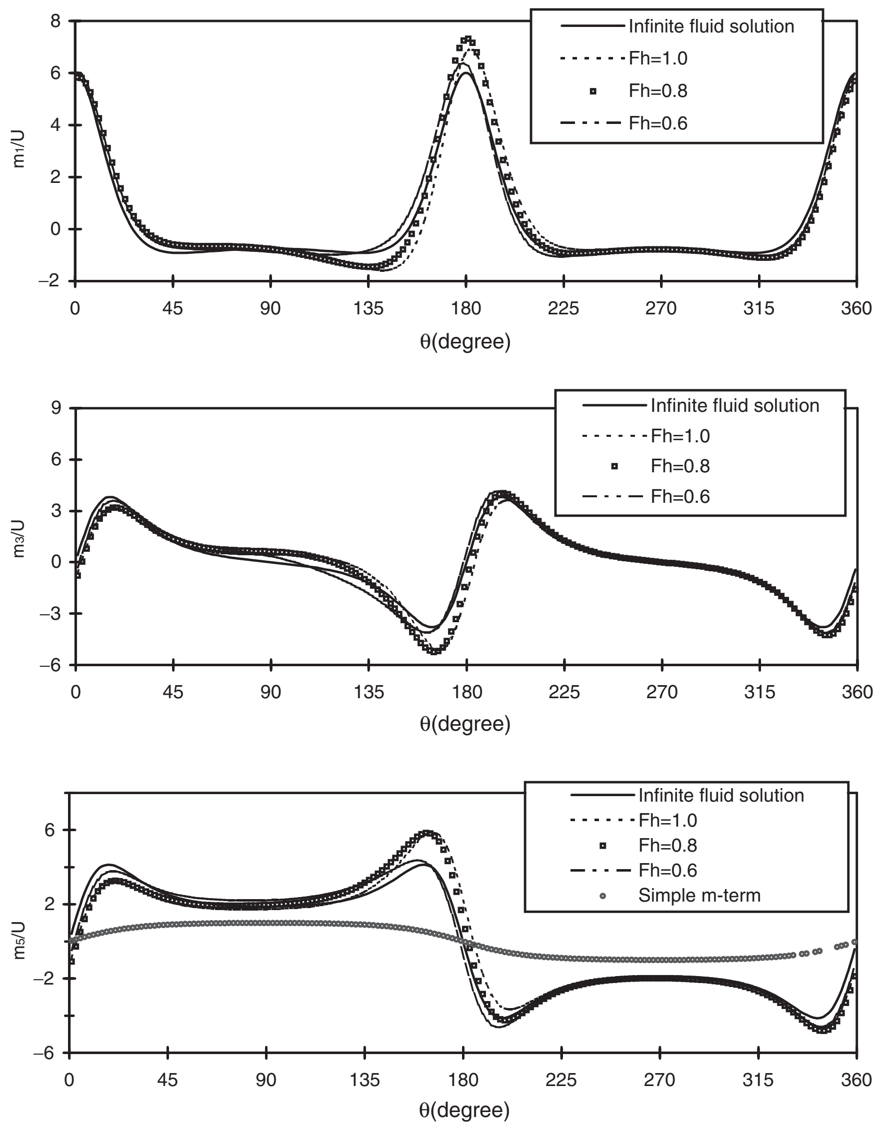

Figure 4. Influence of forward speed on the calculated m-terms associated with an ellipse of dimensions $a/b=2$ at a submerged depth $h=3b$. The infinite fluid solution refers to a deeply submerged ellipse.

purposes. Figure 4 shows that for non-slender bodies this approximation generates large errors over the whole body surface whereas for slender bodies the bow and stern regions are the only areas of concern. Furthermore, overall the calculations for the deeply submerged body or the infinite fluid solution follow similar trends to the other case considered and in particular, its values are comparable with those derived for $F_h=0.6$ indicating that it is an acceptable approximation for the speed range $0 \leqslant F_h \leqslant 0.6$ for elliptic blunt and slender bodies (Figure 6).

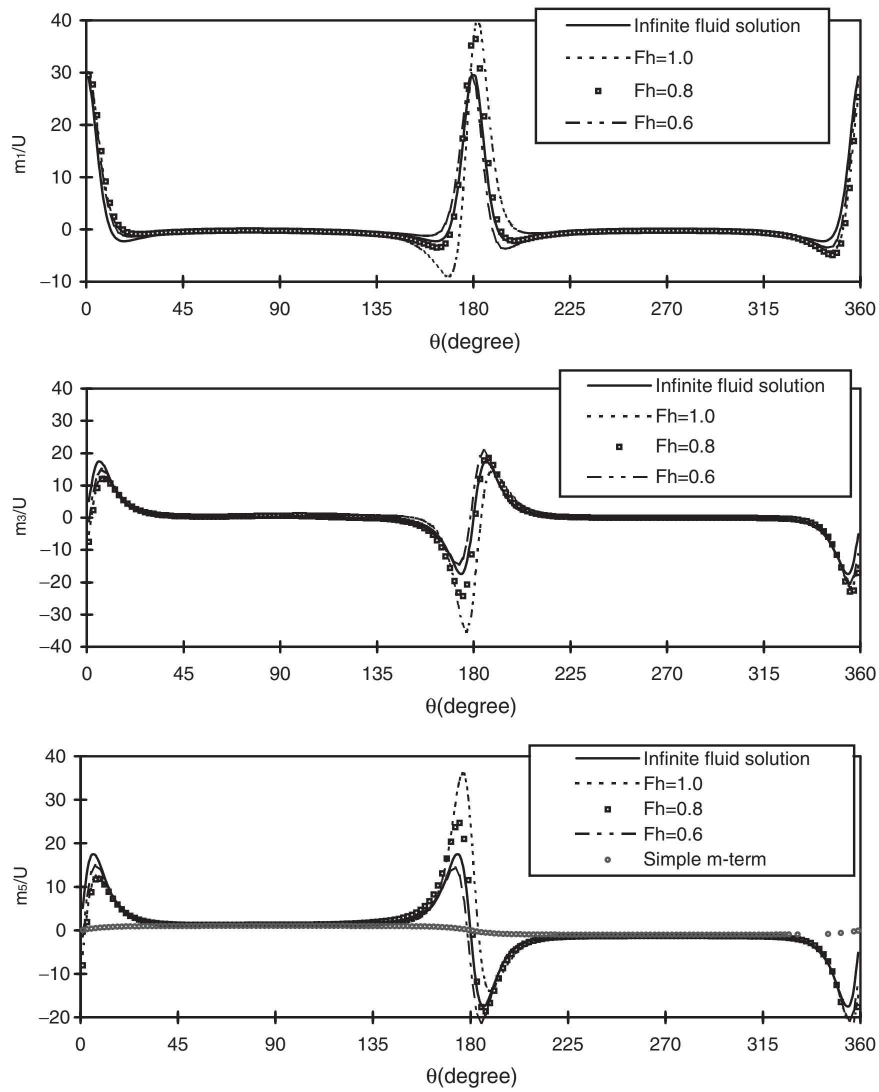

Figure 5. Influence of forward speed on the calculated m-terms associated with an ellipse of dimensions $a/b=5$ at a submerged depth $h=4b$. The infinite fluid solution refers to a deeply submerged ellipse.

6. CONCLUSIONS

An MIEM is proposed for the calculation of the m-terms problem associated with a submerged body advancing near the free surface. This study demonstrates the developed approach to be robust high precision for arbitrary body configurations. Numerical calculations show that for a submerged body, the infinite fluid solution for the m-terms is an engineering approximation for the case of sufficient submerged depth, and the simple theoretical expressions for the

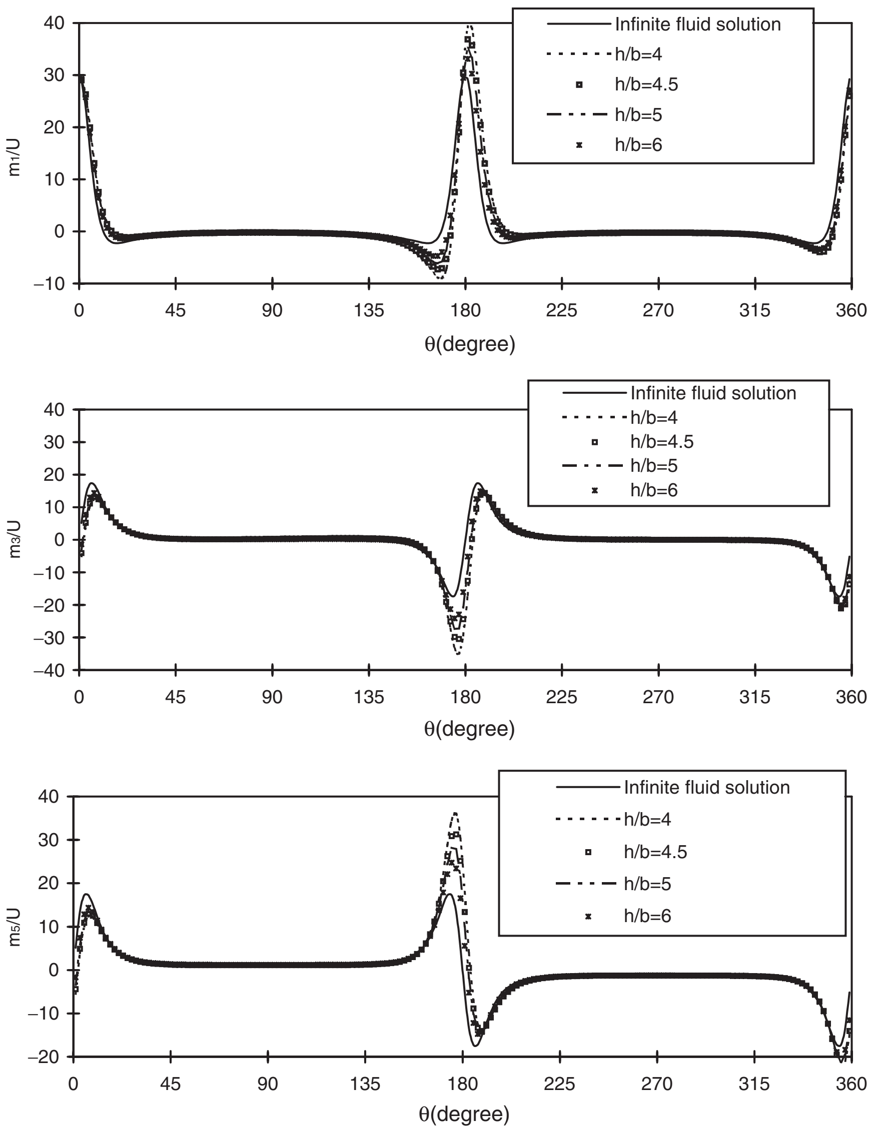

Figure 6. Influence of submerged depth on the calculated m-terms associated with an ellipse of dimensions $a/b=5$ travels with Froude number $F_h=1.0$. The infinite fluid solution refers to a deeply submerged ellipse.

m-terms compared to numerical predictions show marked difference at bow and stern even for a very slender body. For the slender body near a free surface ($h<2a$), wave influences affect the value of the m-terms especially near the bow and stern. This may have important consequences in predicting the pitching motion of the body.

This study requires extension to three-dimensional body forms with numerical simulation combined with unsteady motion prediction.

ACKNOWLEDGEMENTS

This work was supported by the Royal Society Fellowship Scheme, the National Natural Science Foundation of China (N19802008) and the Ministry of Education of China (N199927).

REFERENCES

1. Timman R, Newman JN. The coupled damping coefficients of symmetric ship. *Journal of Ship Research* 1962; **5**(4):34–55.
2. Newman JN. The theory of ship motions. *Advances in Applied Mechanics* 1978; **18**:221–283.
3. Inglis RB, Price WG. The hydrodynamic coefficients of an oscillating ellipsoid moving in the free surface. *Journal of Hydronautics* 1980; **14**(4):105–110.
4. Inglis RB, Price WG. The influence of speed dependent boundary conditions in three dimensional ship motion problems. *International Shipbuilding Progress* 1981; **28**:22–29.
5. Faltinsen OM. *Sea Loads on Ships and Offshore Structures*. Cambridge University Press: Cambridge, 1990.
6. Newman JN. The quest for a three-dimensional theory of ship-wave interactions. *Philosophical Transactions of the Royal Society of London* 1991; **A334**:213–227.
7. Ogilvie TF, Tuck EO. A rational strip theory of ship motions, part one. *Report No*. 013, Department of Naval Architecture and Marine Engineering, University of Michigan, 1969.
8. Beck RF, Magee AR. Time-domain analysis for predicting ship motions. *Proceedings of Symposium on the Dynamics of Marine Vehicles and Structures in Waves*, *Brunel University*, Elsevier: Amsterdam, the Netherlands, 1990.
9. Wu GX. A numerical scheme for calculating the m_j terms in wave-current-body interaction problem. *Applied Ocean Research* 1991; **13**(6):317–321.
10. Duan WY. Theoretical investigation of several ship related problems using a time-domain analysis. *Postdoctoral Research Report of China Ship Scientific Research Center*, WuXi, China, 1998 (in Chinese).
11. Kochin NE, Kibel IA, Roze NV. *Theoretical Hydrodynamics* (Translated from the fifth Russian edition). Interscience: New York, 1964.
12. Wehausen JV, Laitone EV. Surface waves. *Handuck Physik* 1960; **9**:445–778.
13. Lamb H. *Hydrodynamics* (6th edn). Dover Publications Inc.: New York, 1945.
14. Duan WY. Nonlinear hydrodynamic forces acting on a ship undergoing large amplitude motions. *Ph.D. Dissertation*, Department of Naval Architecture and Ocean Engineering, Harbin Engineering University, Harbin, China, 1995 (in Chinese).
15. Abramowitz M, Stegun IA. *Handbook of Mathematical Functions with Formulas*, *Graphs and Mathematical Tables*, Chapter 5. Dover Publications Inc.: New York, 1972.
16. Havelock TH. The forces on a circular cylinder submerged in a uniform stream. *Proceedings of the Royal Society*, *London* 1936; **A157**:526–534.

